

Structural shape parametric optimization for an internal structural-acoustic problem

Christian Soize, J. C. Michelucci

► **To cite this version:**

Christian Soize, J. C. Michelucci. Structural shape parametric optimization for an internal structural-acoustic problem. *Aerospace Science and Technology*, Elsevier, 2000, 4 (-), pp.263-275. 10.1016/S1270-9638(00)00135-8 . hal-00765562

HAL Id: hal-00765562

<https://hal-upec-upem.archives-ouvertes.fr/hal-00765562>

Submitted on 14 Dec 2012

HAL is a multi-disciplinary open access archive for the deposit and dissemination of scientific research documents, whether they are published or not. The documents may come from teaching and research institutions in France or abroad, or from public or private research centers.

L'archive ouverte pluridisciplinaire **HAL**, est destinée au dépôt et à la diffusion de documents scientifiques de niveau recherche, publiés ou non, émanant des établissements d'enseignement et de recherche français ou étrangers, des laboratoires publics ou privés.

Structural shape parametric optimization for an internal structural-acoustic problem

Christian Soize^{a,*}, Jean-Christophe Michelucci^a

^a ONERA, Structural Dynamics and Coupled Systems Department, BP 72, 92322 Châtillon cedex, France

Received 11 May 1999; revised 28 February 2000; accepted 9 March 2000

Abstract

A structural shape optimization problem, with respect to the structural aspect ratio is developed in the context of an axisymmetric structural-acoustic system, consisting of an elastic dome coupled with an internal acoustic cavity, is analyzed in the low- and medium-frequency ranges. The dome is a thin shell considered as a three-dimensional continuum with a dissipative constitutive equation. The internal fluid is a dissipative acoustic field. The dome is submitted to an external wall pressure field modeled by a stochastic field. The cost function is related to the pressure field over an internal axisymmetric observation surface inside the acoustic cavity. We are interested in minimizing the internal noise over the observation surface with respect to the structural aspect ratio defining the geometric shape of the dome. This paper develops an analysis of the structural-acoustic shape optimization problem to determine whether or not there exist values of the dome aspect ratio for which the internal noise is a minimum. The frequency response functions of the structural-acoustic system are calculated to construct the cost function. In this context, the Fourier series expansions of the structural displacement field and the internal fluid velocity potential are carried out with respect to the polar angle variable. For each fixed circumferential wave number, a reduced matrix model is constructed using the structural modes of the structure in vacuo and the acoustic modes of the internal acoustic cavity with rigid wall. The structural modes and the acoustic modes are computed by the finite element method. The optimization parameter is the aspect ratio of the structure. The analysis presented shows that the structural shape optimization problem of the dome with respect to its aspect ratio parameter has a clear solution which minimizes internal noise in the low- and medium-frequency ranges.

shape optimization / structural acoustics / internal noise / acoustics / dynamics / vibration

1. Introduction

This paper deals with a structural shape parametric optimization in the structural-acoustic area. The structure is an elastic dome constituted by an axisymmetric thin shell structure considered as a three-dimensional continuum with a dissipative constitutive equation. The shape of the dome is defined by its aspect ratio which is a scalar parameter. We are interested in the optimization problem with respect to this scalar parameter and not in the general shape optimization [5]. The dome is coupled with an axisymmetric internal dissipative acoustic fluid. The dome is excited by an external random wall pressure field which is stationary in time, such as a wall pressure induced by a turbulent boundary layer due to an external flow. The objective of this paper is only devoted to analyzing the influence of the dome curvature on the coupling mechanism between the structure and the internal acoustic cavity (see below). Consequently, the coupling effects of the structure with the unbounded external acoustic fluid is neglected in order to simplify the parametric analysis. It should be noted that the effects of the external fluid on the structure have two effects [7,12]. The first one is an additional damping for the structure, induced by the acoustic radiation at infinity in the external fluid. This additional damping, which depends on the frequency is smaller than the structural damping and, consequently, does not modify the coupling mechanism between the structure and the internal acoustic cavity. The second effect, which is induced by the external acoustic fluid, is an added mass for the structure. This added mass, which depends on the frequency, generally produces a decreasing of the eigenfrequencies of the structure in a vacuum when the external acoustic fluid is a liquid. This shift effect is significant for the first structural eigenmodes in the LF range. When the modal density of the structure is high enough [10,17], which is the case for the superior part of the LF range and for the MF range of the structure under consideration, the modal density of the structure is not significantly modified, and definitely not sufficiently modified to distort the performed analysis of the coupling mechanism between the structure and the internal acoustic cavity. The observation made on this axisymmetric structural-acoustic system is the internal pressure field over an internal axisymmetric observation surface inside the acoustic cavity. We are interested in minimizing the internal noise over the observation surface with

respect to the geometric shape of the dome defined by its aspect ratio and consequently, the optimization parameter is the aspect ratio of the dome (axisymmetric structure).

The fundamental mechanism induced by the curvature of the dome on the coupling between the structure and the internal acoustic cavity, is the following. The structural membrane waves and the structural flexural waves in the dome are coupled by the curvature of the dome. Structural flexural waves excited by the external wall pressure are converted into structural membrane waves. These structural membrane waves induce a piston movement of the dome nose. This type of structural displacement is associated with a variation in volume of the internal acoustic cavity which induces a high level of internal noise (presently, the observation surface inside the acoustic cavity is not located in the near field of the wall but is located in the far field). This paper develops an analysis of the structural-acoustic shape optimization problem to determine whether or not there exist values of the dome aspect ratio for which the internal noise is a minimum (without, however, developing an automatic optimization algorithm).

Because we are interested in the low- and medium-frequency ranges and taking into account the fact that the dome geometry is not a 'simple shape geometry', the above parametric optimization problem is difficult to solve by analytical methods [3,7,9,13]. This is why the numerical approach proposed in reference [12] is used to solve this internal structural-acoustic optimization problem. According to this reference, in the general case, the modal approach, which is perfectly adapted to the low-frequency range, cannot be extended to the medium-frequency range [12]. However, because the structural-acoustic system considered is axisymmetric, a Fourier series expansion of the response can be made and therefore, the modal approach can still be used for the medium-frequency range which is considered in the application presented in this paper. It should be noted that this method could not be used for a general three-dimensional structural-acoustic system. In addition, in reference [12], the formulation proposed for internal structural-acoustic systems in the low-frequency range differs from the formulation adapted to the medium-frequency range. Since we are not interested in calculation of the structural-acoustic modes and since we wish to use a single formulation for the optimization problem related to the low- and medium-frequency ranges, we chose to use the medium-

frequency model presented in [12]. A reduced matrix model for each fixed circumferential wave number is constructed by a Ritz–Galerkin projection based on the use of the structural modes of the structure in vacuo and the acoustic modes of the internal acoustic cavity with rigid wall. The structural modes and the acoustic modes are computed by the finite element method.

Section 2 is devoted to (1) the geometric description of the three-dimensional axisymmetric structural-acoustic system, (2) its mechanical modeling and the associated three-dimensional boundary value problem, and (3) the Fourier series expansion and the two-dimensional boundary value problems associated with each fixed circumferential wave number. In section 3, we give the variational formulation of the two-dimensional boundary value problem associated with a fixed circumferential wave number. Section 4 is devoted to the construction of the reduced matrix model using the Ritz–Galerkin method. In section 5, we define a normalized power spectral density function of the observation, which is directly used to construct the cost function of the optimization problem. In section 6, we define the optimization problem and we present the method for constructing its solution. Finally, in section 7 we describe a complete numerical application.

2. Three-dimensional axisymmetric structural-acoustic system boundary value problem

2.1. Structural-acoustic system geometry

The geometry of the structural-acoustic system is defined in *figure 1*. The internal acoustic fluid occupies a bounded domain D_F of three-dimensional physical space \mathbb{R}^3 with boundary $\Sigma_F = \Sigma^- \cup \Sigma_F^- \cup \Sigma_F^0$ in which Σ_F^- and Σ_F^0 are rigid walls. The structure occupies a bounded domain D_S of \mathbb{R}^3 with boundary $\Sigma_S = \Sigma^- \cup \Sigma^+ \cup \Sigma_S^0$ in which Σ_S^0 is a rigid wall whereas boundary Σ^- is the coupling interface between the elastic structure and the internal acoustic fluid. The unit normal to Σ_S external to D_S and the unit normal to Σ_F external to D_F are denoted as \mathbf{n} and \mathbf{n}' respectively. Therefore, $\mathbf{n} = -\mathbf{n}'$ on Σ^- . Space \mathbb{R}^3 is referenced to a cartesian reference system $(0, x_1, x_2, x_3)$ also written $(0, x, y, z)$. The generic point of \mathbb{R}^3 is denoted as $\mathbf{x} = (x_1, x_2, x_3)$. We introduce the cylindrical coordinates $(\theta, r, z) \in [0, 2\pi[\times \mathbb{R}^+ \times \mathbb{R}$ such that $x_1 = -r \sin \theta$, $x_2 = r \cos \theta$ et $x_3 = z$. The associated local cylindrical orthonormal basis is $(\mathbf{e}_\theta, \mathbf{e}_r, \mathbf{e}_z)$ as shown in *figure 2*. The coupled system is axisymmetric around axis $(0z)$ as is the internal observation surface Σ . The generating plane is defined by $\{\mathbf{x} \mid x = 0, y > 0\}$. Parts Σ^+ and Σ^- are denoted as Σ^i for i in $\{+, -\}$. The generatrix of Σ^i is denoted as Γ^i and is defined by the function $z \mapsto R^i(z)$. The generatrix Γ of internal observation surface Σ is defined by the function $z \mapsto R(z)$.

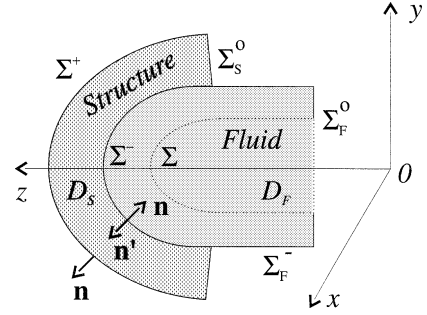


Figure 1. Geometry of the structural-acoustic system.

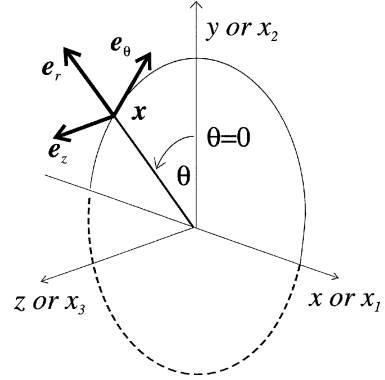


Figure 2. Associated local cylindrical orthonormal basis.

The generating planes of the structure and the internal acoustic fluid are denoted as P_S and P_F respectively. Boundaries Σ_F and Σ_S^0 are generated by curves Γ_F and Γ_S^0 respectively. Let s^i be the curvilinear abscissa of generatrix Γ^i pointing positively in the direction of increasing z . We introduce the curvilinear measure ds^i related to Γ^i and measures $d\Gamma^i$ and $d\Sigma^i$ such that

$$ds^i(z) = (1 + (dR^i(z)/dz)^2)^{1/2} dz, \quad (1)$$

$$d\Gamma^i = R^i(z) ds^i(z), \quad d\Sigma^i = R^i(z) d\theta ds^i(z). \quad (2)$$

For all i in $\{+, -\}$ and all \mathbf{x} in Σ^i , we define a local physical reference system $(\mathbf{b}_1^i = \mathbf{e}_{\theta|_{\Sigma^i}}, \mathbf{b}_2^i = \mathbf{n}^i, \mathbf{b}_3^i = \mathbf{e}_{\theta|_{\Sigma^i}} \wedge \mathbf{n}^i)$ attached to point \mathbf{x} where $\mathbf{n}^+ = \mathbf{n}$ on Σ^+ and $\mathbf{n}^- = -\mathbf{n}$ on Σ^- . The orthogonal 3×3 matrix transforming the local physical reference system into the local cylindrical reference system depends only on z and is written as

$$[\Theta^i(z)] = \begin{bmatrix} 1 & 0 & 0 \\ 0 & \alpha^i(z) & \beta^i(z) \\ 0 & -\beta^i(z) & \alpha^i(z) \end{bmatrix}, \quad (3)$$

$$\alpha^i(z) = (1 + (dR^i(z)/dz)^2)^{-1/2},$$

$$\beta^i(z) = \alpha^i(z) \frac{dR^i(z)}{dz}. \quad (4)$$

2.2. Modeling and boundary value problem of the three-dimensional axisymmetric structural-acoustic system

We consider linear vibrations of the structural-acoustic system around a static equilibrium position without prestresses and taken as reference configuration. The formulation is written in the frequency domain ω (angular frequency in rad/s) for which the Fourier transform convention used is such that, if $t \mapsto f(t)$ is a function from \mathbb{R} into \mathbb{C} , then its Fourier transform is written as $f(\omega) = \int_{\mathbb{R}} e^{-i\omega t} f(t) dt$.

2.2.1. External excitation

The external mechanical excitation applied to the structure is the vector field $\mathbf{x} \mapsto \mathbf{f}(\mathbf{x}, \omega) = -p^+(\mathbf{x}, \omega)\mathbf{n}(\mathbf{x})$ defined on Σ^+ with values in \mathbb{C}^3 .

2.2.2. Internal acoustic fluid

We assume that there is no acoustic source inside acoustic fluid domain D_F . The internal fluid is a dissipative acoustic fluid. Let ρ_0 be the mass density and c_0 the speed of sound in the equilibrium state. The pressure field $p(\mathbf{x}, \omega)$ and the velocity potential $\psi(\mathbf{x}, \omega)$ are such that [11,12]

$$p(\mathbf{x}, \omega) = -i\omega\rho_0\psi(\mathbf{x}, \omega) - \kappa\pi_2(\mathbf{u}), \quad (5)$$

$$\kappa = \frac{\rho_0 c_0^2}{|D_F|}, \quad \pi_2(\mathbf{u}) = \int_{\Sigma^-} \langle \mathbf{u}(\mathbf{x}, \omega), \mathbf{n}'(\mathbf{x}) \rangle d\Sigma^-, \quad (6)$$

in which i denotes the pure imaginary complex number, $\langle \mathbf{u}, \mathbf{v} \rangle = u_1 v_1 + u_2 v_2 + u_3 v_3$, $|D_F| = \int_{D_F} d\mathbf{x}$ is the volume of the internal acoustic cavity and where ψ must satisfy the following constraint equation $\int_{D_F} \psi(\mathbf{x}, \omega) d\mathbf{x} = 0$. It should be noted that in this model, ψ is not exactly a velocity potential because the velocity vector is written as $\mathbf{v}(\mathbf{x}, \omega) = (1 + i\omega\tau)\nabla\psi(\mathbf{x}, \omega)$. The three-dimensional equations for the internal acoustic fluid are written as in [12]

$$\begin{aligned} -\omega^2 \frac{\rho_0}{c_0^2} \psi - i\omega\lambda_0 \rho_0 \nabla^2 \psi - \rho_0 \nabla^2 \psi \\ = -\frac{i\omega\kappa}{c_0^2} \pi_2(\mathbf{u}) \quad \text{in } D_F, \end{aligned} \quad (7)$$

$$\rho_0(1 + i\omega\lambda_0) \frac{\partial \psi}{\partial \mathbf{n}} = i\omega\rho_0 \langle \mathbf{u}, \mathbf{n} \rangle \quad \text{on } \Sigma^-, \quad (8)$$

$$\frac{\partial \psi}{\partial \mathbf{n}} = 0 \quad \text{on } \Sigma_F^+ \cup \Sigma_F^-, \quad (9)$$

$$\int_{D_F} \psi d\mathbf{x} = 0, \quad (10)$$

in which λ_0 is a damping coefficient which may depend on ω . Constraint equation (10) shows that ψ cannot be a constant field.

2.2.3. Structure

The structure is an axisymmetric three-dimensional solid continuum with a linear viscoelastic constitutive equation without memory. Its mass density and its displacement field with values in \mathbb{C}^3 are denoted as $\rho_S(\mathbf{x}) > 0$ and $\mathbf{u}(\mathbf{x}, \omega)$ respectively. The constitutive equation is written as in [12], $\sigma_{jk}(\mathbf{x}, \omega) = \sigma_{jk}^e(\mathbf{x}, \omega) + i\omega\sigma_{jk}^d(\mathbf{x}, \omega)$ in which σ_{jk} is the stress tensor, $\sigma_{jk}^e(\mathbf{x}, \omega) = a_{jkh\ell}(\mathbf{x}) \times \varepsilon_{h\ell}(\mathbf{u})$ is the elastic part of the stress tensor, $\sigma_{jk}^d(\mathbf{x}, \omega) = b_{jkh\ell}(\mathbf{x})\varepsilon_{h\ell}(\mathbf{u})$ is the damping part of the stress tensor and $\varepsilon_{jk} = \frac{1}{2}(\partial_k u_j + \partial_j u_k)$ is the linearized strain tensor in which ∂_k denotes the partial derivative with respect to x_k . Elastic coefficients $a_{jkh\ell}(\mathbf{x})$ and damping coefficients $b_{jkh\ell}(\mathbf{x})$ are real and are assumed to be independent of ω (linear viscoelasticity without memory) in the context of the present shape optimization problem in order to simplify the formulation. These coefficients depend on \mathbf{x} and satisfy the usual symmetry and positivity properties. It is assumed that no external body force field is applied to the structure. In the cartesian reference system and for j and k in $\{1, 2, 3\}$, the elastodynamic equation is written as

$$-\omega^2 \rho_S u_j - \partial_k \sigma_{jk}(\mathbf{u}) = 0 \quad \text{in } D_S, \quad (11)$$

$$u_j = 0 \quad \text{on } \Sigma_S^0, \quad (12)$$

$$\sigma_{jk}(\mathbf{u})n_k = -p_{\Sigma^-} n_k \quad \text{on } \Sigma^-, \quad (13)$$

$$\sigma_{jk}(\mathbf{u})n_k = f_j \quad \text{on } \Sigma^+. \quad (14)$$

2.3. Fourier series expansion and two-dimensional boundary value problem associated with each fixed circumferential wave number

Since the three-dimensional boundary value problem defined in section 2.2 is axisymmetric, a Fourier series expansion of the solution can be made with respect to polar angle θ . This yields a sequence of two-dimensional problems indexed by the circumferential wave number denoted as n . For all n and n' in \mathbb{N} , the orthogonality properties are written as

$$\int_0^{2\pi} \sin n\theta \cos n'\theta d\theta = 0, \quad (15)$$

$$\int_0^{2\pi} \sin n\theta \sin n'\theta d\theta = \delta_{nn'}(1 - \delta_{0n})\pi, \quad (16)$$

$$\int_0^{2\pi} \cos n\theta \cos n'\theta d\theta = \delta_{nn'}(1 + \delta_{0n})\pi, \quad (17)$$

in which $\delta_{nn'} = 0$ if $n \neq n'$ and $\delta_{nn'} = 1$ if $n = n'$.

2.3.1. Structural displacement field

Since the coupled system is axisymmetric, for any fixed r, z and ω , function $\theta \mapsto \mathbf{u}(\theta, r, z, \omega)$ is periodic with period 2π and has the following Fourier series expansion

$$u_\theta(\mathbf{x}, \omega) = \sum_{n=0}^{+\infty} (U_\theta^{(n,s)}(r, z, \omega) \sin n\theta + U_\theta^{(n,as)}(r, z, \omega) \cos n\theta), \quad (18)$$

$$u_r(\mathbf{x}, \omega) = \sum_{n=0}^{+\infty} (U_r^{(n,s)}(r, z, \omega) \cos n\theta - U_r^{(n,as)}(r, z, \omega) \sin n\theta), \quad (19)$$

$$u_z(\mathbf{x}, \omega) = \sum_{n=0}^{+\infty} (U_z^{(n,s)}(r, z, \omega) \cos n\theta - U_z^{(n,as)}(r, z, \omega) \sin n\theta), \quad (20)$$

in which u_θ, u_r and u_z are the components of field \mathbf{u} in the cylindrical basis and where for j in $\{\theta, r, z\}$, n in \mathbb{N} and I in $\{s, as\}$, $U_j^{(n,I)}(r, z, \omega)$ is the complex-valued field defined on $P_S \times \mathbb{R}$. Functions $U_\theta^{(0,s)}, U_r^{(0,as)}$ and $U_z^{(0,as)}$ are equal to zero. Introducing the vector field $\mathbf{U}^{(n,I)} = (U_\theta^{(n,I)}, U_r^{(n,I)}, U_z^{(n,I)})$, equations (18)–(20) can be rewritten as

$$\mathbf{u}(\mathbf{x}, \omega) = \sum_{n=0}^{+\infty} \sum_{I \in \{s, as\}} [F^{(n,I)}(\theta)] \mathbf{U}^{(n,I)}(r, z, \omega), \quad (21)$$

in which, for all θ in $[0, 2\pi]$, matrices $[F^{(n,s)}(\theta)]$ and $[F^{(n,as)}(\theta)]$ are defined by equations (18)–(20). Since we have $[\Theta^i(z)]^T [F^{(n,I)}(\theta)] [\Theta^i(z)] = [F^{(n,I)}(\theta)]$, for any fixed point on surface Σ^+ or Σ^- , structural displacement field \mathbf{u} is also given by equation (21) if it is expressed in the local physical reference system.

2.3.2. Velocity potential of the internal acoustic fluid

The Fourier series expansion of periodic function $\theta \mapsto \psi(\theta, r, z, \omega)$ with period 2π is written as

$$\psi(\theta, r, z, \omega) = \sum_{n=0}^{+\infty} (\Psi^{(n,s)}(r, z, \omega) \cos n\theta - \Psi^{(n,as)}(r, z, \omega) \sin n\theta), \quad (22)$$

where for $n \in \mathbb{N}$ and $I \in \{s, as\}$, the \mathbb{C} -valued two-dimensional field $(r, z) \mapsto \Psi^{(n,I)}(r, z, \omega)$ is defined on $P_F \times \mathbb{R}$. Functions $\Psi^{(0,as)}$ are equal to zero. Equation (22) can be rewritten as

$$\psi(\mathbf{x}, \omega) = \sum_{n=0}^{+\infty} \sum_{I \in \{s, as\}} F^{(n,I)}(\theta) \Psi^{(n,I)}(r, z, \omega), \quad (23)$$

with $F^{(n,s)}(\theta) = \cos n\theta$ and $F^{(n,as)}(\theta) = -\sin n\theta$. Let $\Psi^{(n,s)}$ and $\Psi^{(n,as)}$ be the vector-valued fields defined by $\Psi^{(n,s)} = (-\frac{n}{r}\Psi^{(n,s)}, \partial_r\Psi^{(n,s)}, \partial_z\Psi^{(n,s)})$ and $\Psi^{(n,as)} = (\frac{n}{r}\Psi^{(n,as)}, -\partial_r\Psi^{(n,as)}, -\partial_z\Psi^{(n,as)})$, depending on variables (r, z, ω) . Substituting equations (21) and (23) into equation (5) and using equations (15)–(17) yields

$$p(\mathbf{x}, \omega) = p^{(0)}(r, z, \omega) + \sum_{n=1}^{+\infty} (p^{(n,s)}(r, z, \omega) \cos n\theta - p^{(n,as)}(r, z, \omega) \sin n\theta), \quad (24)$$

$$p^{(0)}(r, z, \omega) = -i\omega\rho_0\Psi^{(0,s)}(r, z, \omega) - \kappa\pi_2(\mathbf{U}^{(0,s)} + \mathbf{U}^{(0,as)}) \quad \text{if } n = 0, \quad (25)$$

$$p^{(n,I)}(r, z, \omega) = -i\omega\rho_0\Psi^{(n,I)}(r, z, \omega) \quad \text{if } n > 0. \quad (25')$$

Substituting equations (21) and (23) into equations (7)–(14) and using equations (15)–(17) yields a sequence of two-dimensional problems indexed by n whose variational formulation is derived below.

3. Variational formulation of the two-dimensional boundary value problem associated with a fixed circumferential wave number

The admissible function space of displacement field $\mathbf{U}^{(n,I)}$ is the complex vector space \mathbb{W}_U of ‘sufficiently differentiable’ function \mathbf{U} defined on P_S with values in \mathbb{C}^3 such that $\mathbf{U} = 0$ on Γ_S^0 . The admissible function space of velocity potential $\Psi^{(n,I)}$ is the complex vector space \mathbb{W}_Ψ of ‘sufficiently differentiable’ function Ψ defined on P_F with values in \mathbb{C} such that $\partial\Psi/\partial\mathbf{n} = 0$ on Γ_F and $\int_{P_F} \Psi(r, z) r dr dz = 0$. For a fixed circumferential wave number n and ω fixed in \mathbb{R} , given $f^{(n,s)}$ and $f^{(n,as)}$, the variational formulation of the two-dimensional problem indexed by n consists in finding $\mathbf{U}^{(n,I)}$ denoted as \mathbf{U} in \mathbb{W}_U and $\Psi^{(n,I)}$ denoted as Ψ in \mathbb{W}_Ψ such that, for all $\delta\mathbf{U}$ in \mathbb{W}_U and for all $\delta\Psi$ in \mathbb{W}_Ψ , we have

$$-\omega^2 m_S^{(n)}(\mathbf{U}, \delta\mathbf{U}) + i\omega c_S^{(n)}(\mathbf{U}, \delta\mathbf{U}) + i\omega a_F^{(n)}(\Psi, \delta\mathbf{U}) + k_S^{(n)}(\mathbf{U}, \delta\mathbf{U}) + \kappa j^{(n)}(\mathbf{U}, \delta\mathbf{U}) = f^{(n,I)}(\omega; \delta\mathbf{U}), \quad (26)$$

$$-\omega^2 m_F^{(n)}(\Psi, \delta\Psi) + i\omega c_F^{(n)}(\omega; \Psi, \delta\Psi) - i\omega a_F^{(n)}(\delta\Psi, \mathbf{U}) + k_F^{(n)}(\Psi, \delta\Psi) = 0, \quad (27)$$

in which the mass, dissipation and stiffness structural bilinear forms are defined by

$$m_S^{(n)}(\mathbf{U}, \delta\mathbf{U}) = (1 + \delta_{0n})\pi \times \int_{P_S} \rho_S \langle \mathbf{U}, \delta\mathbf{U} \rangle r dr dz, \quad (28)$$

$$c_S^{(n)}(\mathbf{U}, \delta\mathbf{U}) = (1 + \delta_{0n})\pi \int_{P_S} \sigma_{jk}^{(n,I),d}(\mathbf{U}) \times \varepsilon_{jk}^{(n,I)}(\delta\mathbf{U}) r dr dz, \quad (29)$$

$$k_S^{(n)}(\mathbf{U}, \delta\mathbf{U}) = (1 + \delta_{0n})\pi \int_{D_S} \sigma_{jk}^{(n,I),e}(\mathbf{U}) \times \varepsilon_{jk}^{(n,I)}(\delta\mathbf{U}) r dr dz, \quad (30)$$

and where $\varepsilon^{(n,I)}$, $\sigma^{(n,I),d}$ and $\sigma^{(n,I),e}$ denote the restriction of the strain tensor, the dissipative part and the elastic part of the stress tensor to \mathbb{W}_U . Concerning the internal acoustic field, we have

$$m_F^{(n)}(\Psi, \delta\Psi) = (1 + \delta_{0n})\pi \frac{\rho_0}{c_0^2} \int_{P_F} \Psi \delta\Psi r dr dz, \quad (31)$$

$$c_F^{(n)}(\omega; \Psi, \delta\Psi) = \lambda_0(\omega) k_F^{(n)}(\Psi, \delta\Psi), \quad (32)$$

$$k_F^{(n)}(\Psi, \delta\Psi) = (1 + \delta_{0n})\pi \rho_0 \int_{P_F} \langle \Psi, \delta\Psi \rangle r dr dz, \quad (33)$$

in which vectors Ψ and $\delta\Psi$ are the vectors associated with Ψ and $\delta\Psi$ as define section 2.3.2. The fluid structure coupling bilinear form $a_F^{(n)}$ and the bilinear form $j^{(n)}$ are define by

$$a_F^{(n)}(\Psi, \delta\mathbf{U}) = -(1 + \delta_{0n})\pi \rho_0 \int_{\Gamma^-} \Psi \langle \delta\mathbf{U}, \mathbf{n} \rangle d\Gamma^-, \quad (34)$$

$$j^{(n)}(\mathbf{U}, \delta\mathbf{U}) = \delta_{0n} 4\pi^2 \pi_2^{(n)}(\mathbf{U}) \pi_2^{(n)}(\delta\mathbf{U}), \quad (35)$$

with

$$\pi_2^{(n)}(\mathbf{U}) = - \int_{\Gamma^-} \langle \mathbf{U}, \mathbf{n} \rangle d\Gamma^-, \quad (36)$$

where $\langle \mathbf{U}, \mathbf{n} \rangle$ denotes the component of vector \mathbf{U} along normal \mathbf{n} on generatrix Γ^+ . The linear form related to the excitation is defined by

$$f^{(n,I)}(\omega; \delta\mathbf{U}) = - \int_{\Gamma^+} \int_0^{2\pi} p^+(\theta, z, \omega) F^{(n,I)}(\theta) d\theta \times \langle \delta\mathbf{U}, \mathbf{n} \rangle(z) d\Gamma^+(z). \quad (37)$$

4. Symmetric reduced matrix model

As explained in section 1, for each fixed circumferential wave number n , a symmetric reduced matrix model of equations (26) and (27) is constructed using the Ritz–Galerkin projection on a finite dimension subspace spanned by a set of structural modes of the structure in vacuo and a set of acoustic modes of the internal acoustic cavity with rigid wall. We then have a sequence of reduced matrix models indexed by n .

4.1. Structural modes of the structure in vacuo

For each fixed n , the structural modes of the structure in vacuo are constructed by finding the eigenvalues $\lambda = \omega^2$ and the associated eigenfunctions $\mathbf{U} \in \mathbb{W}_U$ such that, for all $\delta\mathbf{U}$ in \mathbb{W}_U ,

$$k_S^{(n)}(\mathbf{U}, \delta\mathbf{U}) = \lambda m_S^{(n)}(\mathbf{U}, \delta\mathbf{U}). \quad (38)$$

The spectrum of the eigenvalue problem defined by equation (38) is the countable set $\lambda_{S,\alpha}^{(n)} = (\omega_{S,\alpha}^{(n)})^2$ with $\alpha = 1, 2, \dots$ such that $0 < \omega_{S,1}^{(n)} \leq \omega_{S,2}^{(n)} \leq \dots$ and the associated real-valued eigenfunctions $\mathbf{U}_\alpha^{(n)}$ constitute a complete orthogonal set in \mathbb{W}_U . The normalization of the eigenfunctions are chosen such that $m_S^{(n)}(\mathbf{U}_\alpha^{(n)}, \mathbf{U}_{\alpha'}^{(n)}) = \mu_S \delta_{\alpha\alpha'}$ in which $\mu_S = \int_{D_S} \rho_S d\mathbf{x}$ is the total structural mass. We keep only eigenvectors $\mathbf{U}_\alpha^{(n)}$ whose associated eigenfrequencies $\omega_{S,\alpha}^{(n)}$ lie in the frequency band of analysis denoted as B_0 and which are such that $\int_{\Gamma^-} \langle \mathbf{U}_\alpha^{(n)}, \mathbf{n} \rangle^2 d\Gamma^- \neq 0$. Since there is no internal acoustic excitation but only an external structural excitation, it should be noted that if $\int_{\Gamma^-} \langle \mathbf{U}_\alpha^{(n)}, \mathbf{n} \rangle^2 d\Gamma^- = 0$, then eigenfunction $\mathbf{U}_\alpha^{(n)}$ has a contribution to the response of the structural displacement but no contribution to the pressure response of the internal acoustic cavity (we recall that the cost function of the optimization problem is formulated only in terms of the internal pressure field). For each fixed n , we denote the index set of such eigenfunctions as $\mathcal{J}_S^{(n)} = \{1, \dots, N_S^{(n)}\}$. Consequently, vector field \mathbf{U} as a solution of equations (26) and (27) is written as

$$\mathbf{U}^{(n)}(r, z) \simeq \sum_{\alpha=1}^{N_S^{(n)}} X_{S,\alpha}^{(n)} \mathbf{U}_\alpha^{(n)}(r, z). \quad (39)$$

4.2. Acoustic modes of the internal acoustic cavity with rigid wall

For each fixed n , the acoustic modes of the internal acoustic cavity with rigid wall are constructed by finding the eigenvalues $\lambda = \omega^2$ and the associated eigenfunctions $\Psi \in \mathbb{W}_\Psi$ such that, for all $\delta\Psi$ in \mathbb{W}_Ψ ,

$$k_F^{(n)}(\Psi, \delta\Psi) = \lambda m_F^{(n)}(\Psi, \delta\Psi). \quad (40)$$

The spectrum of the eigenvalue problem defined by equation (40) is the countable set $\lambda_{F,\beta}^{(n)} = (\omega_{F,\beta}^{(n)})^2$ with $\beta = 1, 2, \dots$, such that $0 < \omega_{F,1}^{(n)} \leq \omega_{F,2}^{(n)} \leq \dots$ and the associated real-valued eigenfunctions $\Psi_\beta^{(n)}$ constitute a complete orthogonal set in \mathbb{W}_Ψ . The normalization of the eigenfunctions is chosen such that $m_F^{(n)}(\Psi_\beta^{(n)}, \Psi_{\beta'}^{(n)}) =$

$(\mu_F/c_0^2)\delta_{\beta\beta'}$ in which $\mu_F = \int_{D_F} \rho_0 d\mathbf{x} = \rho_0|D_F|$ is the total mass of the acoustic fluid. We keep only eigenvectors $\Psi_\beta^{(n)}$ whose associated eigenfrequencies $\omega_{F,\beta}^{(n)}$ lie in frequency band B_0 and such that there is an index α in $\mathcal{J}_S^{(n)}$ such that $a_F^{(n)}(\Psi_\beta^{(n)}, \mathbf{U}_\alpha^{(n)}) \neq 0$. If there is no such index α , eigenfunction $\Psi_\beta^{(n)}$ has no contribution to the internal acoustic pressure (see section 4.1). For each fixed n , we denote the index set of such eigenfunctions as $\mathcal{J}_F^{(n)} = \{1, \dots, N_F^{(n)}\}$. Consequently, field Ψ of equations (26) and (27) is written as

$$\Psi^{(n)}(r, z) \simeq \sum_{\beta=1}^{N_F^{(n)}} X_{F,\beta}^{(n)} \Psi_\beta^{(n)}(r, z). \quad (41)$$

4.3. Reduced matrix model for each circumferential wave number

For each fixed n , the restriction of equations (26) and (27) to the subspaces of \mathbb{W}_U and \mathbb{W}_Ψ spanned by the finite families $\{\mathbf{U}_1^{(n)}, \dots, \mathbf{U}_{N_S^{(n)}}^{(n)}\}$ and $\{\Psi_1^{(n)}, \dots, \Psi_{N_F^{(n)}}^{(n)}\}$ respectively yields the reduced matrix model for circumferential wave number n :

$$\begin{aligned} & \left(-\omega^2 \begin{bmatrix} [M_S^{(n)}] & [O_{SF}] \\ [O_{FS}] & -[M_F^{(n)}] \end{bmatrix} \right. \\ & + i\omega \begin{bmatrix} [C_S^{(n)}] & [A_F^{(n)}] \\ [A_F^{(n)T}] & -[C_F^{(n)}] \end{bmatrix} \\ & + \begin{bmatrix} [K_S^{(n)}] & [O_{SF}] \\ [O_{FS}] & -[K_F^{(n)}] \end{bmatrix} \\ & \left. + \kappa \begin{bmatrix} [J^{(n)}] & [O_{SF}] \\ [O_{FS}] & [O_{FF}] \end{bmatrix} \right) \begin{bmatrix} \mathbf{X}_S^{(n,I)}(\omega) \\ \mathbf{X}_F^{(n,I)}(\omega) \end{bmatrix} \\ & = \begin{bmatrix} \mathbf{Y}_S^{(n,I)}(\omega) \\ \mathbf{0} \end{bmatrix}, \quad (42) \end{aligned}$$

in which $\mathbf{X}_S^{(n,I)} = (X_{S,1}^{(n)}, \dots, X_{S,N_S^{(n)}}^{(n)})$ and $\mathbf{X}_F^{(n,I)} = (X_{F,1}^{(n)}, \dots, X_{F,N_F^{(n)}}^{(n)})$ and with

$$[M_S^{(n)}]_{\alpha\alpha'} = m_S^{(n)}(\mathbf{U}_\alpha^{(n)}, \mathbf{U}_{\alpha'}^{(n)}) = \mu_S \delta_{\alpha\alpha'}, \quad (43)$$

$$[C_S^{(n)}]_{\alpha\alpha'} = 2\mu_S \xi_{S,\alpha}^{(n)} \omega_{S,\alpha}^{(n)} \delta_{\alpha\alpha'}, \quad (44)$$

$$[K_S^{(n)}]_{\alpha\alpha'} = k_S^{(n)}(\mathbf{U}_\alpha^{(n)}, \mathbf{U}_{\alpha'}^{(n)}) = \mu_S (\omega_{S,\alpha}^{(n)})^2 \delta_{\alpha\alpha'}, \quad (45)$$

$$[M_F^{(n)}]_{\beta\beta'} = m_F^{(n)}(\Psi_\beta^{(n)}, \Psi_{\beta'}^{(n)}) = (\mu_F/c_0^2) \delta_{\beta\beta'}, \quad (46)$$

$$\begin{aligned} [C_F^{(n)}(\omega)]_{\beta\beta'} &= c_F^{(n)}(\Psi_\beta^{(n)}, \Psi_{\beta'}^{(n)}) \\ &= 2(\mu_F/c_0^2) \xi_{F,\beta}^{(n)} \omega_{F,\beta}^{(n)} \delta_{\beta\beta'}, \quad (47) \end{aligned}$$

$$\begin{aligned} [K_F^{(n)}]_{\beta\beta'} &= k_F^{(n)}(\Psi_\beta^{(n)}, \Psi_{\beta'}^{(n)}) \\ &= (\mu_F/c_0^2) (\omega_{F,\beta}^{(n)})^2 \delta_{\beta\beta'}, \quad (48) \end{aligned}$$

$$[A_F^{(n)}]_{\alpha'\beta} = a_F^{(n)}(\Psi_\beta^{(n)}, \mathbf{U}_{\alpha'}^{(n)}), \quad (49)$$

$$[J^{(n)}]_{\alpha\alpha'} = j^{(n)}(\mathbf{U}_\alpha^{(n)}, \mathbf{U}_{\alpha'}^{(n)}).$$

From equation (35), we deduce that $[J^{(n)}] = [0]$ for all $n \geq 1$. In the context of the present shape optimization problem and in order to simplify the formulation, we assume that the dissipation structural bilinear form is diagonalized by the eigenfunctions $\mathbf{U}_\alpha^{(n)}$. According to the eigenfunction properties introduced in sections 4.1 and 4.2, the coupling matrix is such that, for all $\mathbf{X}_F \in \mathbb{C}^{N_F^{(n)}}$, $[A_F^{(n)}] \mathbf{X}_F = 0 \Rightarrow \mathbf{X} = 0$. Finally, the generalized external structural forces $\mathbf{Y}_S^{(n,I)} = (Y_{S,1}^{(n,I)}, \dots, Y_{S,N_S^{(n)}}^{(n,I)})$ are such that

$$Y_{S,\alpha}^{(n,I)} = f^{(n,I)}(\omega; \mathbf{U}_\alpha^{(n)}). \quad (50)$$

We introduce the generalized dynamic stiffness matrices related to the structure and the internal acoustic fluid:

$$[\mathbb{A}_S^{(n)}(\omega)] = -\omega^2 [M_S^{(n)}] + i\omega [C_S^{(n)}] + [K_S^{(n)}], \quad (51)$$

$$[\mathbb{A}_F^{(n)}(\omega)] = -\omega^2 [M_F^{(n)}] + i\omega [C_F^{(n)}] + [K_F^{(n)}]. \quad (52)$$

5. Normalized power spectral density function of the internal noise observation

In this section, we calculate the normalized power spectral density function of the internal noise observation corresponding to the time-stationary random response of the structural-acoustic system excited by a time-stationary random wall pressure field such as a turbulent boundary layer induced by an external flow. This normalized power spectral density function is related to the spatial average of the quadratic mean of the random internal fluid pressure over observation surface Σ .

5.1. Random wall pressure field excitation

Let E be the mathematical expectation. Random wall pressure field p^+ applied to external structural surface Σ^+ is a second-order real-valued stochastic field $(\mathbf{x}, t) \mapsto p^+(\mathbf{x}, t)$ indexed by $\Sigma^+ \times \mathbb{R}$ which is centered and mean-square stationary with respect to t . In addition, it is assumed that stochastic field p^+ is statistically axisymmetric with respect to surface Σ^+ and we reuse the model introduced in [17]. Let $\tilde{R}_{p^+}(\mathbf{x}, \mathbf{x}', \tau) = E\{p^+(\mathbf{x}, t + \tau)p^+(\mathbf{x}', t)\}$ be its real-valued cross-correlation function which is written as $\tilde{R}_{p^+}(\mathbf{x}, \mathbf{x}', \tau) = \int_{\mathbb{R}} e^{i\omega\tau} \tilde{S}_{p^+}(\mathbf{x}, \mathbf{x}', \omega) d\omega$ where $\tilde{S}_{p^+}(\mathbf{x}, \mathbf{x}', \omega)$ is the

complex-valued cross-spectral density function [8]. For all \mathbf{x} and \mathbf{x}' in Σ^+ , we introduce the notation $S_{p^+}(\theta - \theta', z, z', \omega) = \tilde{S}_{p^+}(\mathbf{x}, \mathbf{x}', \omega)$ and the power spectral density function of the mean-square stationary stochastic process $\{p^+(\mathbf{x}, t), t \in \mathbb{R}\}$ is a positive-valued function defined by $\tilde{\Phi}(\mathbf{x}, \omega) = \tilde{S}_{p^+}(\mathbf{x}, \mathbf{x}, \omega)$ which is independent of θ . Consequently, for all \mathbf{x} fixe in Σ^+ , we have $\tilde{\Phi}(\mathbf{x}, \omega) = \Phi(z, \omega) = S_{p^+}(0, z, z, \omega)$. The cross-spectral density function of p^+ is written as [17]

$$\begin{aligned} S_{p^+}(\theta - \theta', z, z', \omega) \\ = \sqrt{\Phi(z, \omega)\Phi(z', \omega)}G(\xi(z, z'), \eta(\theta - \theta', z, z'), \omega), \end{aligned} \quad (53)$$

in which $\xi(z, z') = s^+(z) - s^+(z')$ with $s^+(z)$ the curvilinear abscissa of generatrix Γ^+ introduced in section 2.1, $\eta(\gamma, z, z') = 0.5(R^+(z) + R^+(z'))g(\gamma)$ with $g(\gamma) = \gamma$ if $-\pi \leq \gamma \leq \pi$, $g(\gamma) = \gamma - 2\pi$ if $\pi < \gamma \leq 2\pi$ and $g(\gamma) = \gamma + 2\pi$ if $-2\pi \leq \gamma < -\pi$. The complex-valued coherence function $G(\xi, \eta, \omega)$ is given by the Corcos model [2] which is written as

$$G(\xi, \eta, \omega) = \exp\left\{i\frac{\xi\omega}{U_c} - \frac{|\xi|}{L_1(\omega)} - \frac{|\eta|}{L_2(\omega)}\right\}, \quad (54)$$

in which $U_c = 0.65U_E$ is the average convection velocity with U_E the average external flow velocity. The longitudinal and lateral correlation scales $L_1(\omega)$ and $L_2(\omega)$ are written as $L_1(\omega) = U_c/(0.115|\omega|)$ and $L_2(\omega) = U_c/(0.7|\omega|)$. For the application presented in section 7, the model used for the power spectral density function $\Phi(z, \omega)$ is written as

$$\begin{aligned} \Phi(z, \omega) = \frac{1}{4000}\rho_0^2 U_E^4 \delta(z)^3 \\ \times \omega^2 (U_E^2 + 25\omega^2 \delta(z)^2)^{-3/2}, \end{aligned} \quad (55)$$

in which $\delta(z)$ is the thickness displacement of the boundary layer.

5.2. Reference power spectral density function

Let $s_{p_{\text{ref}}}^+(\omega)$ be the reference power spectral density function related to surface Σ^+ . Let Π_{Σ^+} be the spatial average over surface Σ^+ of the mean power of stochastic process $\{p^+(\mathbf{x}, t), t \in \mathbb{R}\}$ for \mathbf{x} in Σ^+ . We then have $\Pi_{\Sigma^+} = \int_{\mathbb{R}} s_{p_{\text{ref}}}^+(\omega) d\omega$ in which $s_{p_{\text{ref}}}^+(\omega)$ is the reference power spectral density function defined by

$$s_{p_{\text{ref}}}^+(\omega) = \frac{1}{|\Sigma^+|} \int_{\Sigma^+} \tilde{\Phi}(\mathbf{x}, \omega) d\Sigma^+(\mathbf{x}). \quad (56)$$

5.3. Normalized power spectral density function calculation

From equations (37) and (50), we deduce that

$$\begin{aligned} Y_{S,\alpha}^{(n,I)}(t) = - \int_{\Gamma^+} \int_0^{2\pi} p^+(\theta, z, t) \\ \times F^{(n,I)}(\theta) d\theta \langle \mathbf{U}_\alpha^{(n)}, \mathbf{n} \rangle(z) d\Gamma^+(z), \end{aligned} \quad (57)$$

in the time domain. Therefore, $\mathbf{Y}_S^{(n,I)}(t) = (Y_{S,1}^{(n,I)}(t), \dots, Y_{S,N_S^{(n)}}^{(n,I)}(t))$ is a second-order, centered, mean-square stationary and mean-square continuous stochastic process indexed by \mathbb{R} with values in $\mathbb{R}^{N_S^{(n)}}$. The cross-correlation function of stochastic processes $Y_{S,\alpha}^{(n,I)}(t)$ and $Y_{S,\alpha'}^{(n',I)}(t)$ is defined by

$$R_{Y_{S,\alpha}Y_{S,\alpha'}}^{(n,n',I,I')}(\tau) = E\{Y_{S,\alpha}^{(n,I)}(t+\tau)Y_{S,\alpha'}^{(n',I)}(t)\}, \quad (58)$$

and can be written as

$$R_{Y_{S,\alpha}Y_{S,\alpha'}}^{(n,n',I,I')}(\tau) = \int_{\mathbb{R}} e^{i\omega\tau} S_{Y_{S,\alpha}Y_{S,\alpha'}}^{(n,n',I,I')}(\omega) d\omega, \quad (59)$$

where $S_{Y_{S,\alpha}Y_{S,\alpha'}}^{(n,n',I,I')}(\omega)$ is the cross-spectral density function which can be written as

$$\begin{aligned} S_{Y_{S,\alpha}Y_{S,\alpha'}}^{(n,n',I,I')}(\omega) \\ = 2\pi \delta_{nn'} \delta_{II'} (1 + \delta_{0n}) \\ \times \int_{\Gamma^+} \int_{\Gamma^+} \int_0^\pi S_{p^+}(\gamma, z, z', \omega) \cos n\gamma d\gamma \\ \times \langle \mathbf{U}_\alpha^{(n)}, \mathbf{n} \rangle(z) \langle \mathbf{U}_{\alpha'}^{(n')}, \mathbf{n} \rangle(z') d\Gamma^+(z) d\Gamma^+(z'). \end{aligned} \quad (60)$$

The matrix-valued spectral density function $[S_{\mathbf{Y}_S}^{(n)}(\omega)]$ of vector-valued process $\mathbf{Y}_S^{(n,I)}(t)$ is then defined by $[S_{\mathbf{Y}_S}^{(n)}(\omega)]_{\alpha\alpha'} = S_{Y_{S,\alpha}Y_{S,\alpha'}}^{(n,n,I,I')}(\omega)$.

Let Π_Σ be the spatial average over surface Σ of the mean power of stochastic process $\{p(\mathbf{x}, t), t \in \mathbb{R}\}$ for \mathbf{x} in Σ . From this definition, we deduce that $\Pi_\Sigma = E\{\frac{1}{|\Sigma|} \int_\Sigma p(\mathbf{x}, t)^2 d\Sigma\}$ which can be rewritten as

$$\Pi_\Sigma = \int_{\mathbb{R}} s_{p_\Sigma}(\omega) d\omega, \quad (61)$$

where $s_{p_\Sigma}(\omega)$ is the power spectral density function of the internal noise observation. It is proved [10,17,18] that

$$s_{p_\Sigma}(\omega) = s_0(\omega) + \sum_{n=0}^{+\infty} s_{p_\Sigma}^{(n)}(\omega). \quad (62)$$

The term $s_0(\omega)$ is an additional function induced by the presence of $-\kappa\pi_2$ in equation (5), whose contribution exists only for $n = 0$ and which is written as

$$s_0(\omega) = \frac{8\pi^2\kappa}{|\Sigma|} \text{tr}\{\pi\kappa[S_{\mathbf{X}_S}^{(n)}(\omega)][U_n^{(n)}] - \omega\rho_0\Im m([S_{\mathbf{X}_{SF}}^{(n)}(\omega)][\Upsilon_n^{(n)}])\}, \quad (63)$$

in which $\Im m$ is the imaginary part, tr is the trace operator and $[\Upsilon_n^{(n)}]$ is the matrix defined by

$$[\Upsilon_n^{(n)}]_{\beta\alpha} = \int_{\Gamma} \Psi_{\beta}^{(n)} \int_{\Gamma^-} \langle \mathbf{U}_{\alpha}^{(n)}, \mathbf{n} \rangle d\Gamma^- d\Gamma. \quad (64)$$

The main contributions are the terms $s_{p\Sigma}^{(n)}(\omega)$ which are written as

$$s_{p\Sigma}^{(n)}(\omega) = 2\pi \frac{\omega^2 \rho_0^2}{|\Sigma|} \text{tr}\{[S_{\mathbf{X}_F}^{(n)}(\omega)][\Psi^{(n)}]\}. \quad (65)$$

In equations (63) and (65), we have

$$[S_{\mathbf{X}_F}^{(n)}(\omega)] = [H_{FS}^{(n)}(\omega)][S_{\mathbf{Y}_S}^{(n)}(\omega)][H_{FS}^{(n)}(\omega)]^*, \quad (66)$$

$$[S_{\mathbf{X}_S}^{(n)}(\omega)] = [H_S^{(n)}(\omega)][S_{\mathbf{Y}_S}^{(n)}(\omega)][H_S^{(n)}(\omega)]^*, \quad (67)$$

$$[S_{\mathbf{X}_{SF}}^{(n)}(\omega)] = [H_S^{(n)}(\omega)][S_{\mathbf{Y}_S}^{(n)}(\omega)][H_{FS}^{(n)}(\omega)]^*, \quad (68)$$

$$[H_S^{(n)}(\omega)] = ([\mathbb{A}_S^{(n)}(\omega)] + \kappa[J^{(n)}] - \omega^2[A_F^{(n)}] \times [\mathbb{A}_F^{(n)}(\omega)]^{-1}[A_F^{(n)}]^T)^{-1}, \quad (69)$$

$$[H_{FS}^{(n)}(\omega)] = i\omega[\mathbb{A}_F^{(n)}(\omega)]^{-1}[A_F^{(n)}]^T[H_S^{(n)}(\omega)], \quad (70)$$

$$[H_{SF}^{(n)}(\omega)]^* = -[H_{FS}^{(n)}(\omega)],$$

$$[\Psi^{(n)}]_{\beta\beta'} = \int_{\Gamma} \Psi_{\beta}^{(n)} \Psi_{\beta'}^{(n)} d\Gamma, \quad (71)$$

$$[U_n^{(n)}]_{\alpha\alpha'} = \int_{\Gamma} \int_{\Gamma^-} \langle \mathbf{U}_{\alpha}^{(n)}, \mathbf{n} \rangle d\Gamma^- \times \int_{\Gamma^-} \langle \mathbf{U}_{\alpha'}^{(n)}, \mathbf{n} \rangle d\Gamma^- d\Gamma. \quad (72)$$

Finally, the normalized power spectral density function of the internal noise observation is defined by

$$s_{p\Sigma, \text{norm}}(\omega) = \frac{s_{p\Sigma}(\omega)}{s_{p_{\text{ref}}^+}(\omega)}. \quad (73)$$

It should be noted that $[\mathbb{A}_F^{(n)}(\omega)]$ is a diagonal matrix and consequently, the inverse matrix which appears in equations (69) and (70) is explicitly known.

6. Shape optimization with respect to the aspect ratio of the dome

6.1. Class of geometry

The objective is to optimize the dome shape in order to minimize the noise related to observation surface Σ located inside the internal acoustic cavity. Since we are looking for the influence of the dome curvature, all the other main parameters of the structural acoustic system (volume of the internal acoustic cavity, external structural surface area, dome thickness and constitutive material) have to remain constant when the shape of the dome is modified in the dome-shape optimization process. The external power injected in the structural-acoustic system is proportional to the external structural surface area on which the external random wall pressure field excitation is applied. Since we are only interested in analyzing the influence of the dome curvature on the internal noise, this surface area has to remain a constant in order to not introduce a strong variation of the external power input when the dome shape is modified. The volume of the internal acoustic cavity is a constant for that the modal density of the internal acoustic cavity be nearly a constant when the dome shape is modified. In addition, since the dome thickness is very small compared to the other structural-acoustic system dimensions, the area of internal structural surface Σ^- is almost equal to the area of external structural surface Σ^+ . The internal generatrix $\Gamma^- \cup \Gamma_F^-$ is chosen as an arc of an ellipse, possibly extended by a line segment of a line parallel to axis (0z) and belonging to the generative plane. This ellipse is centered in the reference system origin and characterized by its semiminor axis which has a fixed value a_{ref} and its semimajor axis b (see figures 3 and 4). The characteristic ratio of the ellipse is defined by $q = b/a_{\text{ref}}$. Each value of characteristic ratio q define a geometric configuration of the structural-acoustic system and q is called the structural aspect ratio. Figures 3 and 4 define the z-axes, denoted as $z_a, z_b, z_c, z_d = b$ and z_e , of all

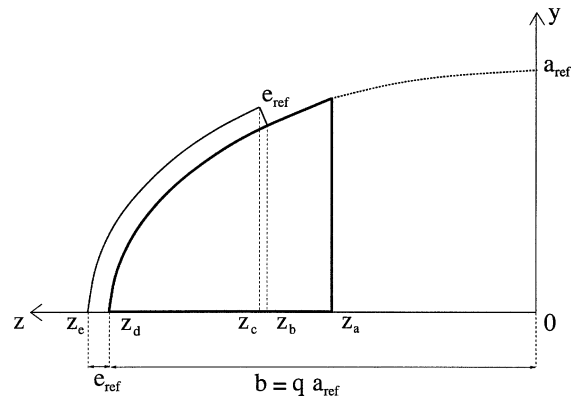


Figure 3. Geometry of the generative plane: case of an arc of the ellipse.

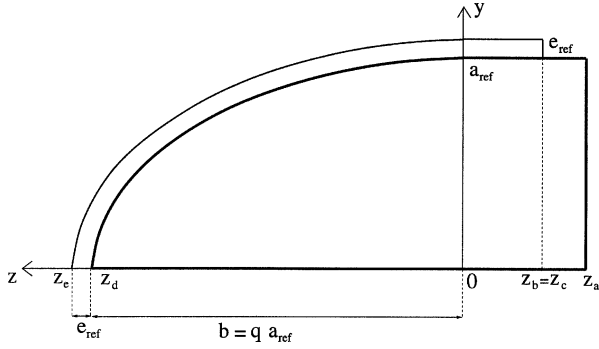


Figure 4. Geometry of the generative plane: case of a quarter of the ellipse extended by a line segment.

the particular points which allow the geometry of the structure and the internal acoustic cavity to be defined. Figures 3 and 4 correspond to $z_a > 0$ (an arc of the ellipse) and $z_a < 0$ (a quarter of the ellipse extended by a line segment) respectively. The internal acoustic cavity is located between z_a and $z_d = b$. The length of the internal acoustic cavity is denoted as ℓ and is such that $\ell = z_d - z_a = b - z_a$. The constraint $|\Sigma^-|$ remains a constant defined by the value of z_b . A reference configuration is defined by a given value $q_{\text{ref}} > 1$ of structural aspect ratio q . For all values of q , the structure thickness is a constant e_{ref} corresponding to the reference configuration. We have $z_e = z_d + e_{\text{ref}}$.

6.2. Optimization problem with respect to the aspect ratio of the dome

6.2.1. Optimization parameter

Structural aspect ratio $q > 0$ takes its values in an interval denoted as \mathcal{Q} and define by

$$\mathcal{Q} =]0, 2q_{\text{ref}}[. \quad (74)$$

The values of q such that $0 < q < 1$, $q = 1$ and $1 < q < 2q_{\text{ref}}$ correspond to a dome which is not slender, one which is part of a sphere, and one which is a slender structure respectively.

6.2.2. Cost function

The analysis is made over the frequency bands $B_1 = [1, 1500]$ Hz and $B_2 = [1, 500]$ Hz. Given index $i = 1, 2$, the cost function $q \mapsto J_{\Sigma}^{(i)}(q)$ from \mathcal{Q} into $]0, +\infty[$ is defined for each frequency band B_i by

$$J_{\Sigma}^{(i)}(q) = \frac{1}{|B_i|} \int_{B_i} s_{p\Sigma, \text{norm}}(\omega) d\omega, \quad (75)$$

in which $s_{p\Sigma, \text{norm}}(\omega)$ is the normalized power spectral density function related to the observation surface Σ

and which is defined by equation (73) as a function of structural aspect ratio q .

6.2.3. Optimization problem

Given the frequency band B_i , the optimization problem associated with cost function $q \mapsto J_{\Sigma}^{(i)}(q)$ consists in finding $q^{(i)}$ in \mathcal{Q} such that

$$J_{\Sigma}^{(i)}(q^{(i)}) = \min_{q \in \mathcal{Q}} J_{\Sigma}^{(i)}(q). \quad (76)$$

6.2.4. Solution method and structural shape parametric optimization

Each value of q in \mathcal{Q} defines a geometric configuration which has to be modeled by the finite element method. Consequently, for each given structural aspect ratio q , a finite element mesh of the dome and a finite element mesh of the internal acoustic cavity have to be constructed, then the structural modes and the acoustic modes have to be calculated before starting to compute the cost function for the value of q considered. It should be noted that the cost function is strongly nonlinear with respect to parameter q and a sensitivity analysis [6] is not adapted to the problem under consideration. For a given value of q , an examination of the numerical cost induced by computation of the cost function (and possibly of its derivative with respect to q) shows that the use of an automatic optimization algorithm [4, 14–16, 19] would lead to a very high numerical cost, probably with some serious numerical difficulties. In addition, we are interested not only in the optimum value of the structural aspect ratio but also in performing the structural shape parametric optimization; that is to say, in knowing the variation of the cost function as a function of q in order to identify the domain of q for which the internal noise could be high. Consequently, we have chosen a very simple method (which is perfectly adapted to the problem and very efficient in this case), consisting in constructing the graph of the cost function q by q and then identifying the minimum value of the cost function by looking at its graph. Taking into account the high numerical cost for computing one value of the cost function, interval \mathcal{Q} is discretized by a ‘reasonable’ number of discrete values of q .

7. Numerical results

7.1. Numerical data

7.1.1. Structure

The structure is made of a composite material modeled as a linear isotropic homogeneous material with density $\rho_S = 1750$ kg/m³, Young’s modulus $E_S = 1.615 \cdot 10^{10}$ N/m², Poisson’s ratio $\nu_S = 0.137$ and dissipation coefficient $\xi_S = 0.02$.

The reference geometric configuration is defined by $a_{\text{ref}} = 3.13$ m, $q_{\text{ref}} = 3.6$ (therefore, $b_{\text{ref}} = 11.26$ m), $l_{\text{ref}} = 4.29$ m, structure thickness $e_{\text{ref}} = 0.027$ m and $|\Sigma^+|_{\text{ref}} = 50.6$ m². For each value of q , a finite element mesh of the structure (generative plane) is constructed using parabolic finite elements with 8 nodes. The thickness (smallest dome dimension) is discretized into two finite element layers. The finite element type and the number of layers were determined from studying the result of convergence of all the eigenfunctions and eigenvalues corresponding to the extreme configuration $q = 7.0$ which leads to the greatest number of modes within frequency band $B_0 = [1, 2000]$ Hz. For the extreme geometric configurations corresponding to $q = 0.3$ and $q = 7.0$, the number of finite elements and the number of nodes are 616–2469 and 892–3573 respectively.

7.1.2. Internal acoustic fluid

The internal acoustic fluid is water with density $\rho_0 = 1000$ kg/m³, speed of sound $c_0 = 1500$ m/s and dissipation coefficient $\xi_{F,\beta}^{(n)} = 0.01$ for every acoustic mode. The acoustic cavity volume $|D_F|_{\text{ref}}$ of the reference geometric configuration is assigned the value 64 m³. For each value of q , a finite element mesh (compatible with the structure) of the internal acoustic cavity (generative plane) is constructed using linear triangular finite elements. For the extreme geometric configurations corresponding to $q = 0.3$ and $q = 7.0$, the number of finite elements and the number of nodes are 8694–4499 and 13663–7073 respectively. The uniform distance between boundary $\Sigma^- \cup \Sigma_F^-$ and observation surface Σ is equal to $0.6a_{\text{ref}}$.

7.1.3. Data for the excitation corresponding to a random wall pressure field

The parameter values of the model defined by equations (53)–(55) are $U_E = 7.5$ m/s and $\delta(z) = \delta_{\text{max}}(z_e - z)/(z_e - z_c)$ with $\delta_{\text{max}} = 5.1 \cdot 10^{-3}$ m.

7.2. Structural shape parametric optimization results

In order to decrease the numerical cost due to the optimization procedure, the non usual additional terms induced by the presence of $-\kappa\pi_2$ in equation (5), whose contribution exists only for $n = 0$, are not taken into account in the numerical calculation. It should be noted that the coupling terms (see equations (26) and (27)) between the structure and the internal acoustic cavity, represented by bilinear form $a_F^{(n)}(\Psi, \mathbf{U})$ defined by equation (34), are always kept in the numerical calculation.

7.2.1. Eigenmode extraction and convergence computation

The finite element meshes used for the structure and the internal acoustic cavity allow us to compute the eigen-

modes whose associated eigenfrequencies are in the frequency band $[1, 2000]$ Hz. The structural modes and acoustic modes are computed by the subspace iteration method [1] checking Sturm's sequence, using an accelerated scheme for convergence and a Lanczos method for initialization. For each circumferential wave number n , the reduced matrix model uses the structural modes and acoustic modes whose eigenfrequencies are in frequency band $B_0 = [1, 2000]$ Hz; this ensures that power spectral density functions $\omega \mapsto s_{p\Sigma}^{(n)}(\omega)$ defined by equation (65) are uniformly converged over frequency band $B_1 = [1, 1500]$ Hz. An analysis was carried out [10] to study the convergence of normalized power spectral density function $s_{p\Sigma, \text{norm}}$ defined by equation (73) with respect to circumferential wave number n . This analysis shows that uniform convergence over frequency band $B_1 = [1, 1500]$ Hz is achieved when contributions $n = 0, 1, 2, 3, 4, 5$ are taken into account. For instance, figure 5 shows the variation of $\mapsto J_{\Sigma}^{(1)}(1)$ as a function of n .

7.2.2. Optimization results

Let us introduce the frequency moving average of normalized power spectral density function $s_{p\Sigma, \text{norm}}$, defined by

$$\langle s_{p\Sigma, \text{norm}} \rangle_{\Delta f}(\omega) = \frac{1}{\Delta\omega} \int_{\omega - \Delta\omega/2}^{\omega + \Delta\omega/2} s_{p\Sigma, \text{norm}}(\omega') d\omega',$$

in which $\Delta\omega = 2\pi\Delta f$. The following numerical results were obtained [10] for $\Delta f = 100$ Hz: figures 6 to 9 show the graphs of functions $\omega \mapsto \langle s_{p\Sigma, \text{norm}} \rangle_{\Delta f}(\omega)$ expressed in Hz for several values of structural aspect ratio q ; figures 10 and 11 show the graphs of cost functions $q \mapsto J_{\Sigma}^{(1)}(q)$ and $q \mapsto J_{\Sigma}^{(2)}(q)$ for frequency bands B_1 and B_2 respectively. It can be seen that for the two frequency

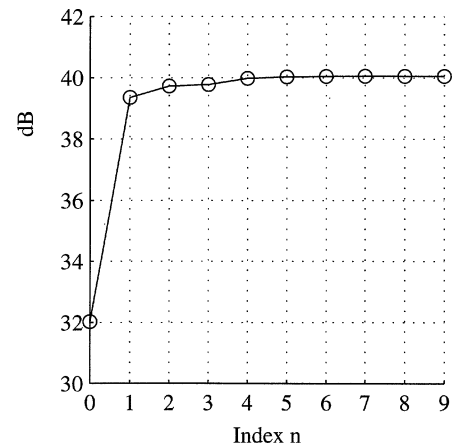


Figure 5. Convergence: variation of $10 \times \log_{10}(J_{\Sigma}^{(1)}(1)/10^{-18})$ as a function of n .

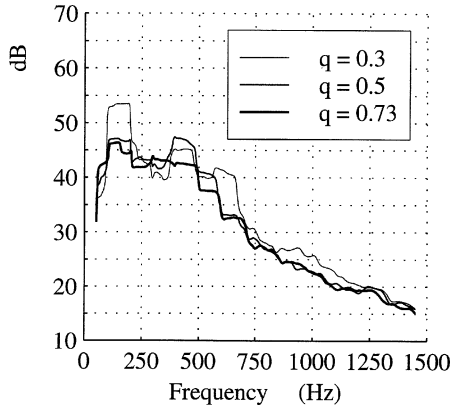


Figure 6. Graphs of functions $\omega \mapsto 10 \times \log_{10}(\langle s_{p_{\Sigma}, \text{norm}} \rangle_{100}(\omega) / 10^{-18})$ for structural aspect ratio $q = 0.3$ (thin solid line), 0.5 (medium solid line), 0.73 (thick solid line).

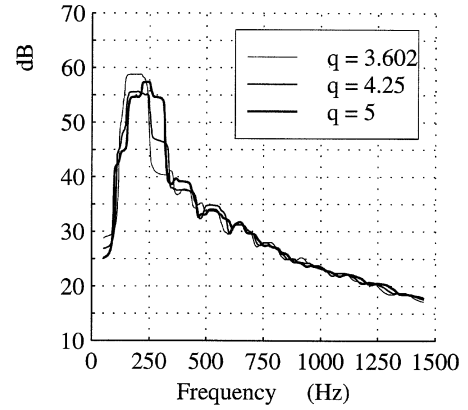


Figure 9. Graphs of functions $\omega \mapsto 10 \times \log_{10}(\langle s_{p_{\Sigma}, \text{norm}} \rangle_{100}(\omega) / 10^{-18})$ for structural aspect ratio $q = 3.602$ (thin solid line), 4.25 (medium solid line), 5.0 (thick solid line).

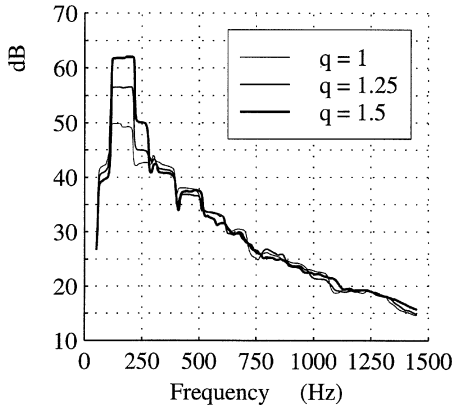


Figure 7. Graphs of functions $\omega \mapsto 10 \times \log_{10}(\langle s_{p_{\Sigma}, \text{norm}} \rangle_{100}(\omega) / 10^{-18})$ for structural aspect ratio $q = 1.0$ (thin solid line), 1.25 (medium solid line), 1.5 (thick solid line).

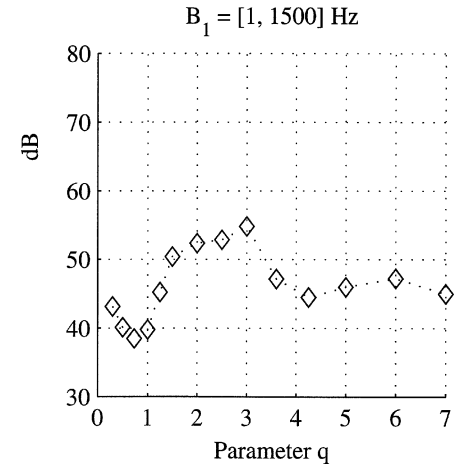


Figure 10. Graph of cost function $q \mapsto 10 \times \log_{10}(J_{\Sigma}^1(q) / 10^{-18})$ for frequency band $B_1 = [1, 1500]$ Hz.

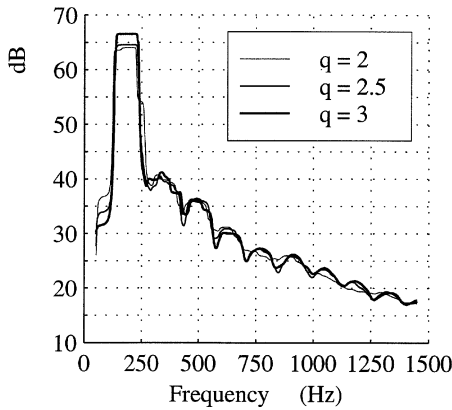


Figure 8. Graphs of functions $\omega \mapsto 10 \times \log_{10}(\langle s_{p_{\Sigma}, \text{norm}} \rangle_{100}(\omega) / 10^{-18})$ for structural aspect ratio $q = 2.0$ (thin solid line), 2.5 (medium solid line), 3.0 (thick solid line).

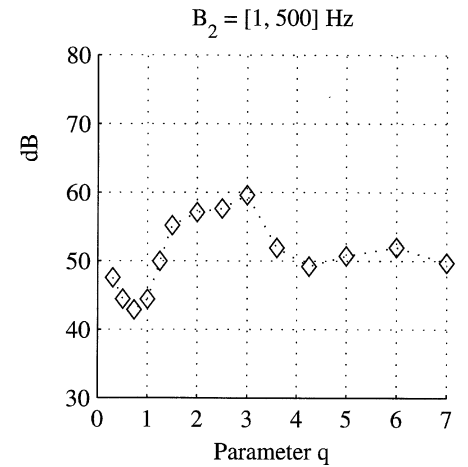


Figure 11. Graph of cost function $q \mapsto 10 \times \log_{10}(J_{\Sigma}^2(q) / 10^{-18})$ for frequency band $B_2 = [1, 500]$ Hz.

bands, the lowest energy level occurs when $q = 0.73$. Nevertheless, it should be noted that the minimum value obtained for $q = 0.73$ differs by only about 1 dB from the energy level obtained for $q = 1.0$. The highest energy levels are obtained for q belonging to the range [1.5, 3.5].

8. Conclusions

The analysis presented in this paper shows that the structural shape optimization of a dome with respect to its aspect ratio, excited by an external random wall pressure field, has a clear solution which minimizes internal noise in the low- and medium-frequency ranges. This solution corresponds to structural aspect ratios belonging to subinterval [0.7, 1.0]. In addition, this analysis shows that internal noise is high in the low- and medium-frequency ranges when the structural aspect ratio belongs to subinterval [1.5, 3.5] which should be avoided.

References

- [1] Bathe K.J., Wilson E.L., Numerical Methods in Finite Element Analysis, Prentice Hall, New York, 1976.
- [2] Corcos G.M., The structure of the turbulent pressure field in boundary layer flows, *J. Fluid Mech.* 18 (1964) 353–378.
- [3] Fahy F., Sound and Structural Vibration, Academic Press, London, 1987.
- [4] Fletcher R., Practical Methods of Optimization – Vol. 2, Constrained Optimization, Wiley, New York, 1980.
- [5] Haslinger J., Neittaanmaki P., Finite Element Approximation for Optimal Shape, Material and Topology Design, Second Edition, John Wiley, Chichester, 1996.
- [6] Haug E.J., Choi K.K., Komkov V., Design Sensitivity Analysis of Structural Systems, Academic Press, 1986.
- [7] Junger M.C., Feit D., Sound, Structures and their Interaction, Acoust. Soc. Am. Publications on Acoustics, Woodbury, 1993 (originally published MIT Press, Cambridge, 1972).
- [8] Krée P., Soize C., Mathematics of Random Phenomena, Reidel, Dordrecht, 1983.
- [9] Lesueur C., Rayonnement Acoustique des Structures, Eyrolles, Paris, 1988.
- [10] Michelucci J.-C., Optimisation de forme structurale axisymétrique en vibroacoustique interne dans les domaines des basses et moyennes fréquences, Doctorat de l'École Centrale Paris, 1998.
- [11] Morand H.J.-P., Ohayon R., Fluid Structure Interaction, Wiley, New York, 1995.
- [12] Ohayon R., Soize C., Structural Acoustics and Vibration, Academic Press, London, 1998.
- [13] Pierce A.D., Acoustics: An Introduction to its Physical Principles and Applications, Acoust. Soc. Am. Publications on Acoustics, Woodbury, 1989 (originally published McGraw-Hill, New York, 1981).
- [14] Polak E., Computational Methods in Optimization, Academic Press, New York, 1971.
- [15] Powell M.J.D., Nonlinear Optimization, Academic Press, New York, 1981.
- [16] Sewell M.J., Maximum and Minimum Principles, Cambridge University Press, Cambridge, 1987.
- [17] Soize C., Desanti A., David J.-M., Dynamic and acoustic response of coupled structure-dense fluid axisymmetric systems excited by a random wall pressure field, *Rech. Aérospatiale* 5 (1989) 1–13.
- [18] Soize C., The Fokker–Planck Equation for Stochastic Dynamical Systems and its Explicit Steady State Solutions, World Scientific, Singapore, 1994.
- [19] Walter E., Pronzato L., Identification of Parametric Models from Experimental Data, Springer-Verlag, Berlin, 1997.